

Critical exponents of the semimetal-insulator transition in graphene: A Monte Carlo study

Joaquín E. Drut¹ and Timo A. Lähde²

¹*Department of Physics, The Ohio State University, Columbus, Ohio 43210-1117, USA*

²*Department of Physics, University of Washington, Seattle, Washington 98195-1560, USA*

(Received 8 May 2009; published 25 June 2009)

The low-energy theory of graphene exhibits spontaneous chiral symmetry breaking due to pairing of quasiparticles and holes, corresponding to a semimetal-insulator transition at strong Coulomb coupling. We report a lattice Monte Carlo study of the critical exponents of this transition as a function of the number of Dirac flavors N_f , finding $\delta=1.25 \pm 0.05$ for $N_f=0$, $\delta=2.26 \pm 0.06$ for $N_f=2$ and $\delta=2.62 \pm 0.11$ for $N_f=4$, with $\gamma \simeq 1$ throughout. We compare our results with recent analytical work for graphene and closely related systems and discuss scenarios for the fate of the chiral transition at finite temperature and carrier density, an issue of relevance for upcoming experiments with suspended graphene samples.

DOI: 10.1103/PhysRevB.79.241405

PACS number(s): 73.63.Bd, 71.30.+h, 05.10.Ln

Graphene, a single layer of carbon atoms arranged in a honeycomb lattice,^{1,2} provides a building block for more complex allotropes such as graphite (graphene sheets attached by van der Waals forces), fullerenes (graphene spheres with pentagonal dislocations), and nanotubes (cylindrically rolled-up graphene). In the absence of electron-electron interactions, the valence and conduction bands of graphene are connected by two inequivalent “Dirac points” around which the low-energy excitations are massless quasiparticles with a linear dispersion relation and a Fermi velocity of $v_F \simeq c/300$.^{3,4} Such a semimetallic band structure is, unfortunately, unsuitable for many electronic applications, which depend crucially on the ability to externally modify the conduction properties, as routinely done with semiconducting devices. The quest to engineer a band gap in graphene has thus been propelled to the forefront of current research. Hitherto suggested solutions include gap formation due to interaction with a substrate,⁴ induction of strain,⁵ and geometric confinement by means of nanoribbons or quantum dots.⁶

The low v_F in graphene indicates that the analog of the fine-structure constant of Quantum electrodynamics (QED) is $\alpha_g \sim 1$, and thus the Coulomb attraction between electrons and holes may play a significant role in defining the ground-state properties. An intriguing possibility is that spontaneous formation of excitons (electron-hole bound states) and the concomitant breaking of chiral symmetry may turn graphene into a Mott insulator. While the strength of the Coulomb interaction precludes a perturbative approach, previous (approximate) analytic studies⁷ at the neutral point (zero carrier density n) and zero temperature T have addressed the appearance of an excitonic gap as a function of α_g (see Fig. 1). Such treatments suggest that the transition into the insulating phase should be governed by essential singularities rather than power laws, a behavior known as Miransky scaling.⁸

In our recent lattice Monte Carlo (LMC) study,⁹ indications were found that the chiral transition is of second order, with well-defined critical exponents. Subsequently, in Ref. 10 we provided a rough estimate of the critical exponents as $\delta \sim 2.3$, $\beta_m \sim 0.8$, and $\gamma \simeq 1$, although a more precise determination was not possible due to insufficient data on large-enough lattices. Nevertheless, Miransky scaling and classical mean-field exponents were found to be disfavored.

The aim of the present work is to provide a more rigorous

and comprehensive determination of the quantum critical properties for $N_f=0, 2$, and 4 Dirac flavors, as well as to contrast these results with recent analytical and simulational work for graphene and related theories. We also briefly elaborate on the mechanisms that inhibit exciton formation at nonzero T and n and their connection to other systems.

The LMC studies of Refs. 9–11 suggest that the low-energy theory of graphene is an appropriate starting point for a quantitative analysis. This is defined by the Euclidean action

$$S_E = - \int d^2x dt \bar{\psi}_a D[A_0] \psi_a + \frac{\epsilon_0}{2e^2} \int d^3x dt (\partial_t A_0)^2, \quad (1)$$

with the Dirac operator

$$D[A_0] = \gamma_0(\partial_0 + iA_0) + v \gamma_i \partial_i + m_0, \quad i = 1, 2, \quad (2)$$

where the ψ_a with $a=1, \dots, N_f$ are four-component spinors in 2+1 dimensions, A_0 is a Coulomb field in 3+1 dimensions, and the case of a graphene monolayer is recovered for $N_f=2$ in the limit $m_0 \rightarrow 0$. Furthermore, $\alpha_g \equiv e^2/(4\pi v \epsilon_0)$ with the inverse coupling $\beta \equiv v \epsilon_0/e^2$ such that screening by a substrate is reflected in the dielectric constant ϵ_0 .

The gauge term of Eq. (1) is discretized in the noncompact formulation.^{9,10} The staggered discretization¹² of the fermionic component of Eq. (1) is preferred as chiral symmetry is then partially retained at finite lattice spacing. As N staggered flavors correspond to $N_f=2N$ continuum Dirac flavors,¹³ the case of $N_f=2$ is recovered for $N=1$, giving

$$S_E^f[\bar{\chi}, \chi, U_0] = - \sum_{m,n} \bar{\chi}_m K_{m,n}[U_0] \chi_n, \quad (3)$$

where the χ_n are staggered fermion spinors and the site indices (m, n) are restricted to a 2+1 dimensional sublattice. Invariance under spatially uniform, time-dependent gauge transformations is retained by the link variables $U_{0,n} = U_n \equiv \exp(i\theta_n)$, where θ_n is the lattice gauge field. For $v=1$, the staggered form of Eq. (2) is

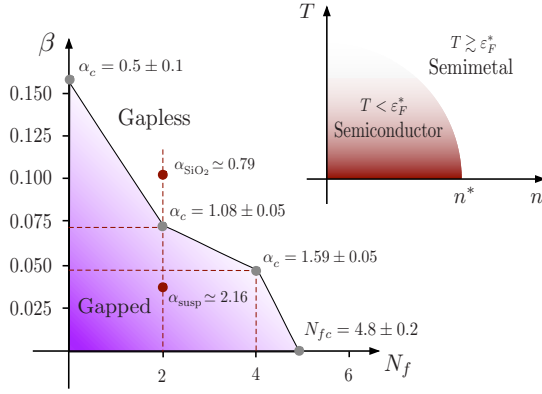


FIG. 1. (Color online) Phase diagram in the $(N_f$ and β) plane. The gapped phase is bounded by a critical Coulomb coupling $\alpha_c \equiv (4\pi\beta_c)^{-1}$ and a critical number of fermion flavors N_{fc} . The coupling on a SiO₂ substrate is denoted by α_{SiO_2} and for suspended graphene by α_{susp} . Inset: hypothetical phase diagram in the $(n$ and T) plane. At low T , suspended graphene exhibits semimetallic properties whenever the carrier density n exceeds a characteristic value n^* . At the neutral point the semiconducting behavior persists until $T \approx \varepsilon_F^* = \hbar v_F \sqrt{\pi n^*}$, where the transition may be of Berezinskii-Kosterlitz-Thouless type or a crossover.

$$K_{m,n}[U] = \frac{1}{2} [\delta_{m+e_0,n} U_m - \delta_{m-e_0,n} U_n^\dagger] + \frac{1}{2} \sum_i \eta_{i,m} [\delta_{m+e_i,n} - \delta_{m-e_i,n}] + m_0 \delta_{m,n}, \quad (4)$$

where $\eta_{1,n} = (-1)^{n_0}$ and $\eta_{2,n} = (-1)^{n_0+n_1}$. Our simulations use the hybrid Monte Carlo (HMC) algorithm with N pseudofermion flavors on a 2+1 dimensional space-time lattice of extent L such that θ also propagates in the third spatial dimension of extent L_z . Further details are given in Refs. 10 and 14.

We now seek to characterize the critical exponents of the chiral transition in graphene. The spontaneous breakdown of chiral symmetry in Eq. (1) is signaled by a nonzero condensate $\sigma \equiv \langle \bar{\chi} \chi \rangle$. The mass term in Eq. (2) breaks chiral symmetry explicitly, generating a nonvanishing condensate, which is otherwise not possible at finite volume. The appearance of a gap in the quasiparticle spectrum of graphene at a critical coupling β_c is then marked by $\sigma \neq 0$ for $m_0 \rightarrow 0$. However, the ‘‘chiral limit’’ $m_0 \rightarrow 0$ cannot be approached directly as that limit corresponds to a very large fermionic correlation length, especially in the vicinity of β_c due to the appearance of Goldstone modes. Practical simulations are performed at finite m_0 such that the limit $m_0 \rightarrow 0$ is reached by extrapolation for which it is useful to also study the susceptibility $\chi_l \equiv \partial \sigma / \partial m_0$ and the logarithmic derivative $R \equiv \partial \ln \sigma / \partial \ln m_0$. An instructive way to determine β_c and the critical exponents is by fitting an equation of state (EOS) $m_0 = f(\sigma, \beta)$ to simulation data at finite m_0 . Knowledge of $f(\sigma, \beta)$ with good precision close to the transition then allows for an educated extrapolation to the chiral limit.

We have considered the EOS successfully applied¹⁵ to lattice QED,

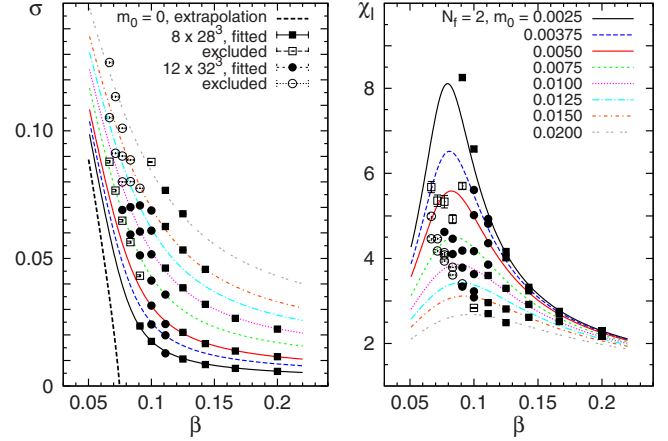


FIG. 2. (Color online) Chiral condensate σ (left panel) and susceptibility χ_l (right panel) for $N_f=2$. Data for $L=28$, $L_z=8$ are indicated by squares and for $L=32$, $L_z=12$ by circles. The lines represent a χ^2 fit to σ and χ_l and extrapolation $m_0 \rightarrow 0$ using Eq. (5). The open data points are excluded due to finite-volume or lattice spacing effects. The optimal fit is $\beta_c = 0.0738 \pm 0.0010$ and $\delta = 2.23 \pm 0.06$, with $X_0 = 0.36 \pm 0.05$, $X_1 = -0.13 \pm 0.02$, and $Y_1 = -0.15 \pm 0.02$. The errors are of statistical origin. The method of analysis is described in detail in Refs. 9 and 10.

$$m_0 X(\beta) = Y(\beta) f_1(\sigma) + f_3(\sigma), \quad (5)$$

where $X(\beta)$ and $Y(\beta)$ are expanded around β_c such that $X(\beta) = X_0 + X_1(1 - \beta/\beta_c)$ and $Y(\beta) = Y_1(1 - \beta/\beta_c)$. The dependence on σ is given by $f_1(\sigma) = \sigma^b$ and $f_3(\sigma) = \sigma^\delta$, where $b \equiv \delta - 1/\beta_m$. The critical exponents are

$$\beta_m \equiv \left. \frac{\partial \ln \sigma}{\partial \ln(\beta_c - \beta)} \right|_{m_0=0}^{\beta/\beta_c}, \quad (6)$$

and

$$\gamma \equiv \left. \frac{\partial \ln \chi_l}{\partial \ln(\beta_c - \beta)} \right|_{m_0=0}^{\beta/\beta_c}, \quad \delta \equiv \left[\left. \frac{\partial \ln \sigma}{\partial \ln m_0} \right]^{-1} \right|_{m_0 \rightarrow 0}^{\beta=\beta_c}, \quad (7)$$

which are assumed to obey the hyperscaling relation $\beta_m(\delta - 1) = \gamma$. It should also be noted that $R \rightarrow 1/\delta$ for $m_0 \rightarrow 0$ at $\beta = \beta_c$. Our results and analyses in terms of Eq. (5) are shown in Fig. 2 for $N_f=2$, in Fig. 3 for $N_f=4$, and for the quenched case $N_f=0$ in Fig. 4. All of our results are consistent with $b = 1.00 \pm 0.05$; hence, we conclude that $\gamma \approx 1$ based on the hyperscaling relation such that the remaining exponent to determine is δ . Based on the EOS analysis and the logarithmic derivative R (see Fig. 5), we find $\delta = 2.26 \pm 0.06$ for $N_f=2$, $\delta = 2.62 \pm 0.11$ for $N_f=4$, and $\delta = 1.25 \pm 0.05$ for $N_f=0$. We observe that finite-volume effects decrease with increasing N_f and that data points for small β and large m_0 in the broken phase are not well described by Eq. (5), likely due to a small correlation length associated with a growing excitonic gap.

An increase in δ with N_f is consistent with the LMC results of Ref. 11 where a similar trend was found, culminating at $3.6 \leq \delta \leq 6$ for $N_f = N_{fc} \approx 4.8$ where the chiral transition disappears. Such behavior is reminiscent of the Thirring

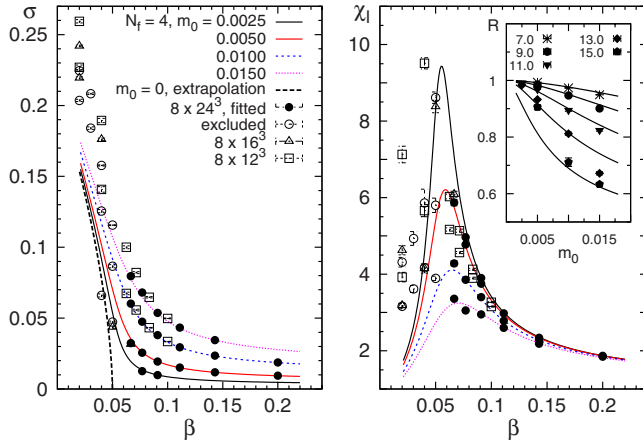


FIG. 3. (Color online) Chiral condensate σ (left panel) and susceptibility χ_l (right panel) for $N_f=4$ for lattices up to $L=24$, $L_z=8$. Inset: logarithmic derivative R for different β^{-1} . The optimal fit is $\beta_c=0.0499 \pm 0.0010$ and $\delta=2.62 \pm 0.11$, with $X_0=0.19 \pm 0.05$, $X_1=-0.09 \pm 0.02$, and $Y_1=-0.08 \pm 0.02$. See also Fig. 2.

model in 2+1 dimensions,¹⁶ where $\delta \approx 2.8$ for $N_f=2$, reaching $\delta \approx 7$ at a critical flavor number of $N_{fc} \approx 6.6$. Extensive LMC studies of QED have found $\delta \approx 2.2$ for $N_f=0$,¹⁷ while for QED with dynamical fermions $\delta \approx 3$.¹⁵ The case of QED in 2+1 dimensions (QED₃) is noteworthy as the LMC study of Ref. 18 yielded $\delta \approx 2.3$ for $N_f=1$ and $\delta \approx 2.7$ for $N_f=4$, which are suggestive of our values for graphene, although spontaneous chiral symmetry breaking in QED₃ is difficult to establish as the order parameter can be exponentially suppressed for large N_f .

The gap-equation analysis of Ref. 7 reported $\beta_c \approx 0.16$ for $N_f=0$ and $\beta_c \approx 0.066$ for $N_f=2$, which are in qualitative agreement with our results. However, the transition of Ref. 7 is of infinite order and vanishes for $N_f=4$. These discrepancies are smallest for $N_f=0$, where our results approach $\delta=1$. Our observations are thus in line with indications¹⁹ that the critical exponents, as obtained from Schwinger-Dyson equa-

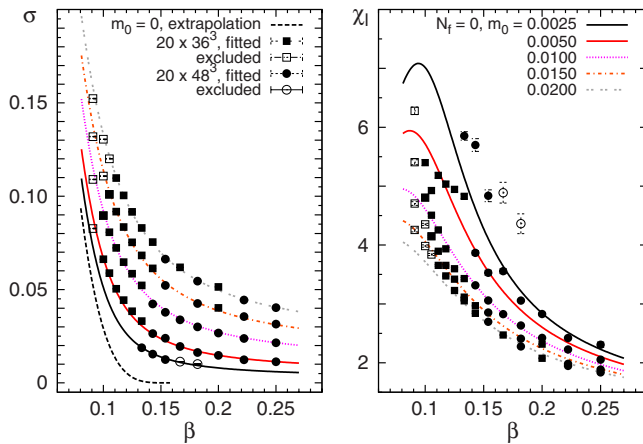


FIG. 4. (Color online) Chiral condensate σ (left panel) and susceptibility χ_l (right panel) for $N_f=0$, with $L=36$, $L_z=20$ (squares) and $L=48$, $L_z=20$ (circles). The optimal fit with fixed $\delta=1.25$ is $\beta_c=0.158 \pm 0.001$, with $X_0=0.16 \pm 0.02$, $X_1=-0.10 \pm 0.05$, and $Y_1=-0.11 \pm 0.02$. The range $\delta=1.25 \pm 0.05$ yields $\beta_c=0.16 \pm 0.02$.

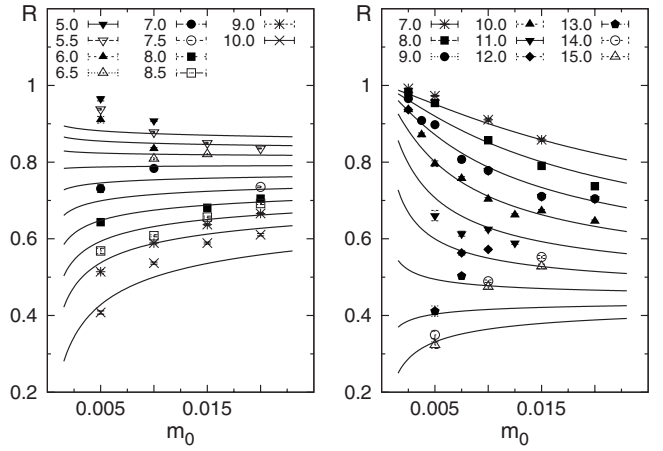


FIG. 5. Logarithmic derivative R for $N_f=0$ (left panel) and $N_f=2$ (right panel) for different β^{-1} . The data for $N_f=0$ indicate that $\delta \approx 1.2$, while the case of $N_f=2$ is compatible with $\delta \approx 2.2$. Finite-volume effects are substantial for $N_f=0$ at large β and small m_0 .

tion (SDE) analyses, may be dependent on the chosen resummation scheme.

An effective theory containing both the order parameter and the Dirac quasiparticles as dynamical fields has recently been developed in Ref. 20. Based on an expansion to leading order around $\epsilon=3-d$ spatial dimensions, the long-range $\sim 1/r$ Coulomb tail was found to be irrelevant in the renormalization group (RG) sense such that the chiral transition could then be described using only short-range interactions of the Gross-Neveu-Yukawa form, yielding the estimates $\gamma \sim 1.25$ and $\delta \sim 2.8$ for the critical exponents at $N_f=2$, in qualitative agreement with our present findings, as well as with large- N_f calculations of the RG flow.²¹ However, our results are not compatible with $\delta=2+O(1/N_f)$ found in Refs. 20 and 22, which is surprising as the Gross-Neveu-Yukawa theory is expected to interpolate between $\delta=19/5 \approx 4$ at $N_f=0$ and $\delta=2$ in the $N_f \rightarrow \infty$ limit.²⁰ It is not clear, as no chiral transition exists in the graphene theory above the critical flavor number $N_{fc}=4.8$,¹¹ how to consistently compare our results with large- N_f estimates.

What is the fate of the semimetal-insulator transition at nonzero temperature? On the basis of the Mermin-Wagner theorem,²³ one expects either a crossover or a Berezinskii-Kosterlitz-Thouless (BKT) transition²⁴ at a critical temperature T_c . The most compelling experimental evidence so far for a BKT transition has been reported in Ref. 25, where graphene samples on a substrate were subjected to transverse magnetic fields up to $B \approx 30$ T. In the temperature range of 10–1 K, a growth in the resistivity by a factor of ~ 200 was observed and attributed to the “magnetic catalysis” predicted in Refs. 26 and 27. At $B=0$, the resistivity of annealed suspended graphene was observed²⁸ to increase by a factor of ~ 3 over a temperature range of 200–50 K while also changing character from metallic to semiconducting. A study of the low-energy theory of graphene at nonzero T is thus clearly called for, possibly along the lines of Ref. 29, which considered the Gross-Neveu model in 2+1 dimensions.

At low T , the large extent of the imaginary time dimension renders the system effectively three dimensional such

that a chiral transition may still be observed at a critical density n^* . Interestingly, away from the neutral (unpolarized) point, nonrelativistic Fermi systems (such as the asymmetric Fermi liquid in the context of ultracold atoms and dilute neutron matter³⁰) can undergo transitions into exotic phases^{31–33} before reverting to a fully polarized normal state. Whether the low-energy theory of graphene exhibits such phenomena is currently unknown.

We acknowledge support under U.S. DOE (Grants No. DE-FG-02-97ER41014, No. DE-FG02-00ER41132, and No.

DE-AC02-05CH11231), UNEDF SciDAC Collaboration (Grant No. DE-FC02-07ER41457), and NSF (Grant No. PHY-0653312). J.E.D. acknowledges the hospitality of the Institute for Nuclear Theory during the completion of this work. This work was supported in part by an allocation of computing time from the Ohio Supercomputer Center. We thank A. Bulgac and M. J. Savage for computer time, and R. J. Furnstahl, S. J. Hands, I. Herbut, and D. T. Son for valuable comments.

- ¹K. S. Novoselov, A. K. Geim, S. V. Morozov, D. Jiang, Y. Zhang, S. V. Dubonos, I. V. Grigorieva, and A. A. Firsov, *Science* **306**, 666 (2004); *Proc. Natl. Acad. Sci. U.S.A.* **102**, 10451 (2005); *Nature (London)* **438**, 197 (2005); A. K. Geim and K. S. Novoselov, *Nature Mater.* **6**, 183 (2007).
- ²A. H. Castro Neto, F. Guinea, N. M. R. Peres, K. S. Novoselov, and A. K. Geim, *Rev. Mod. Phys.* **81**, 109 (2009).
- ³S. Y. Zhou, G.-H. Gweon, A. V. Fedorov, P. N. First, W. A. de Heer, D.-H. Lee, F. Guinea, A. H. Castro Neto, and A. Lanzara, *Nature Mater.* **6**, 770 (2007); A. Bostwick, T. Ohta, T. Seyller, K. Horn, and E. Rotenberg, *Nat. Phys.* **3**, 36 (2007); G. Li, A. Luican, and E. Y. Andrei, *Phys. Rev. Lett.* **102**, 176804 (2009).
- ⁴S. Y. Zhou, D. A. Siegel, A. V. Fedorov, and A. Lanzara, *Physica E* **40**, 2642 (2008); *Nature Mater.* **7**, 259 (2008).
- ⁵T. Yu *et al.*, *J. Phys. Chem. C* **112**, 12602 (2008); Z. H. Ni, T. Yu, Y. H. Lu, Y. Y. Wang, Y. P. Feng, and Z. X. Shen, *ACS Nano* **3**, 483 (2009); V. Pereira and A. Castro Neto, arXiv:0810.4539 (unpublished); V. Pereira, A. Castro Neto, and N. Peres, arXiv:0811.4396 (unpublished).
- ⁶Y.-W. Son, M. L. Cohen, and S. G. Louie, *Phys. Rev. Lett.* **97**, 216803 (2006); L. Yang, C.-H. Park, Y.-W. Son, M. L. Cohen, and S. G. Louie, *ibid.* **99**, 186801 (2007); B. Sahu, H. Min, A. H. MacDonald, and S. K. Banerjee, *Phys. Rev. B* **78**, 045404 (2008).
- ⁷D. V. Khveshchenko, *Phys. Rev. Lett.* **87**, 246802 (2001); *J. Phys.: Condens. Matter* **21**, 075303 (2009); D. V. Khveshchenko and H. Leal, *Nucl. Phys. B* **687**, 323 (2004).
- ⁸P. I. Fomin, V. P. Gusynin, V. A. Miransky, and Yu. A. Sitenko, *Nucl. Phys. B* **110**, 445 (1976); *Riv. Nuovo Cimento* **6**, N. 5, Ser. 3, 1 (1983); V. A. Miransky, *Nuovo Cimento Soc. Ital. Fis., A* **90**, 149 (1985).
- ⁹J. E. Drut and T. A. Lähde, *Phys. Rev. Lett.* **102**, 026802 (2009).
- ¹⁰J. E. Drut and T. A. Lähde, *Phys. Rev. B* **79**, 165425 (2009); A. H. Castro Neto, *Physics* **2**, 30 (2009).
- ¹¹S. J. Hands and C. G. Strouthos, *Phys. Rev. B* **78**, 165423 (2008).
- ¹²J. Kogut and L. Susskind, *Phys. Rev. D* **11**, 395 (1975); L. Susskind, *ibid.* **16**, 3031 (1977); H. Kluberg-Stern, *Nucl. Phys. B* **220**, 447 (1983).
- ¹³C. Burden and A. N. Burkitt, *Europhys. Lett.* **3**, 545 (1987).
- ¹⁴H. J. Rothe, *Lattice Gauge Theories—An Introduction*, 3rd ed. (World Scientific, Singapore, 2005).
- ¹⁵M. Göckeler, R. Horsley, E. Laermann, P. Rakow, G. Schierholz, R. Sommer, and U.-J. Wiese, *Nucl. Phys. B* **334**, 527 (1990); M. Göckeler, R. Horsley, P. Rakow, G. Schierholz, and R. Sommer, *ibid.* **371**, 713 (1992); M. Göckeler, R. Horsley, V. Linke, P. E. L. Rakow, G. Schierholz, and H. Stüben, *ibid.* **487**, 313 (1997).
- ¹⁶S. Christofi, S. Hands, and C. Strouthos, *Phys. Rev. D* **75**, 101701(R) (2007).
- ¹⁷A. Kocić, J. B. Kogut, M.-P. Lombardo, and K. C. Wang, *Nucl. Phys. B* **397**, 451 (1993).
- ¹⁸S. J. Hands, J. B. Kogut, L. Scorzato, and C. G. Strouthos, *Phys. Rev. B* **70**, 104501 (2004).
- ¹⁹K. Kondo, Y. Kikukawa, and H. Mino, *Phys. Lett. B* **220**, 270 (1989); M. Gomes, R. S. Mendes, R. F. Ribeiro, and A. J. da Silva, *Phys. Rev. D* **43**, 3516 (1991); D. K. Hong and S. H. Park, *ibid.* **49**, 5507 (1994).
- ²⁰I. Herbut, V. Juričić, and O. Vafek, arXiv:0904.1019 (unpublished).
- ²¹I. L. Aleiner, D. E. Kharzeev, and A. M. Tsvelik, *Phys. Rev. B* **76**, 195415 (2007); J. E. Drut and D. T. Son, *ibid.* **77**, 075115 (2008).
- ²²I. F. Herbut, *Phys. Rev. Lett.* **97**, 146401 (2006).
- ²³N. D. Mermin and H. Wagner, *Phys. Rev. Lett.* **17**, 1133 (1966); P. C. Hohenberg, *Phys. Rev.* **158**, 383 (1967); S. Coleman, *Commun. Math. Phys.* **31**, 259 (1973).
- ²⁴S. L. Sondhi, S. M. Girvin, J. P. Carini, and D. Shahar, *Rev. Mod. Phys.* **69**, 315 (1997).
- ²⁵J. G. Checkelsky, L. Li, and N. P. Ong, *Phys. Rev. B* **79**, 115434 (2009).
- ²⁶D. V. Khveshchenko, *Phys. Rev. Lett.* **87**, 206401 (2001).
- ²⁷E. V. Gorbar, V. P. Gusynin, V. A. Miransky, and I. A. Shovkovy, *Phys. Rev. B* **66**, 045108 (2002); V. P. Gusynin, V. A. Miransky, S. G. Sharapov, and I. A. Shovkovy, *ibid.* **74**, 195429 (2006); **77**, 205409 (2008).
- ²⁸K. I. Bolotin, K. J. Sikes, J. Hone, H. L. Stormer, and P. Kim, *Phys. Rev. Lett.* **101**, 096802 (2008); V. Crespi, *Physics* **1**, 15 (2008).
- ²⁹S. J. Hands, J. B. Kogut, and C. G. Strouthos, *Phys. Lett. B* **515**, 407 (2001).
- ³⁰D. T. Son and M. A. Stephanov, *Phys. Rev. A* **74**, 013614 (2006); A. Bulgac and M. McNeil Forbes, *ibid.* **75**, 031605(R) (2007); R. Sharma and S. Reddy, *ibid.* **78**, 063609 (2008); S. Giorgini, L. P. Pitaevskii, and S. Stringari, *Rev. Mod. Phys.* **80**, 1215 (2008).
- ³¹P. Fulde and R. A. Ferrell, *Phys. Rev.* **135**, A550 (1964); A. I. Larkin and Y. N. Ovchinnikov, *Sov. Phys. JETP* **20**, 762 (1965).
- ³²G. Sarma, *J. Phys. Chem. Solids* **24**, 1029 (1963).
- ³³W. V. Liu and F. Wilczek, *Phys. Rev. Lett.* **90**, 047002 (2003).